Influence of the multilayer dielectric mirror design on the laser damage growth in the sub-picosecond regime

Saaxewer Diop, Marine Chorel, Éric Lavastre, Nadja Roquin, Laurent Gallais, Nicolas Bonod, Laurent Lamaignère

Influence of the multilayer dielectric mirror design on the laser damage growth in the sub-picosecond regime

Saaxewer Diop[1,2,*], Marine Chorel[1], Éric Lavastre[1], Nadja Roquin[1], Laurent Gallais[2], Nicolas Bonod[2], and Laurent Lamaignère[1]

[1] *Commissariat à l'Énergie Atomique et aux Énergies Alternatives - Centre d'Études Scientifiques et Techniques d'Aquitaine (CEA-CESTA), F-33116 Le Barp, France*
[2] *Aix-Marseille Univ, CNRS, Centrale Marseille, Institut Fresnel, 13013 Marseille, France*
[*] *Corresponding author: saaxewer.diop@cea.fr*

Compiled March 13, 2024

The peak-power on high-power laser facilities is limited by the laser-induced damage on the final optical components. Also, when a damage site is generated, the damage growth phenomenon limits the lifetime of the component. Many studies have been performed to improve the laser-induced damage threshold of these components. The question now arises as to whether an improvement of the initiation threshold leads to a reduction of the damage growth phenomenon. To address this question, we performed damage growth experiments on three different multilayer dielectric mirror designs exhibiting different damage thresholds. We used a classical quarter-wave designs and optimized designs. The experiments were carried out with a spatially top-hat beam, spectrally centered at 1053 nm with a pulse duration of 0.8 ps in *s*- and *p*-polarization. The results evidenced the impact of design on the improvement of the damage growth thresholds and a reduction of the damage growth rates. A numerical model was used to simulate damage growth sequences. The results reveal similar trends to those observed experimentally. On the basis of these three cases, we have shown that an improvement of the initiation threshold through a modification of the mirror design can lead to a reduction of the damage growth phenomenon.

http://dx.doi.org/10.1364/ao.XX.XXXXXX

1. INTRODUCTION

The peak power of petawatt-class lasers has steadily increased since the development of the Chirped Pulse Amplification (CPA) technique [1]. However, the peak-power remains limited by the laser-induced damage on the final optical components of these facilities [2]. Laser-induced damage is driven by non-linear photo-ionizations in the sub-picosecond regime. These phenomena lead to the critical electron density of the material which triggers the damage mechanism [3–6]. The mechanisms imply that the damage threshold is linked to the intrinsic properties of the material, notably the bandgap energy [7, 8]. Several studies have improved the understanding of damage mechanisms on Multilayer Dielectric (MLD) coatings which depend on different laser parameters such as the pulse duration for example [9–11].

Laser-Induced Damage Threshold (LIDT) improvement of optical components of high-power laser facilities is not sufficient to avoid the occurrence of damage sites because of defects due to manufacturing process and of particle contamination [12–17]. The initial size of these damage sites is generally micrometric which is too small to have detrimental effects on the beam propagation. However, a significant increase of the damaged area has been reported after successive shots [18–20]. The determination the growth threshold and the damage growth rate is an important issue to predict the lifetime of these components.

In the sub-picosecond regime, laser-induced damage has a deterministic behavior, and LIDT depends on the Electric Field Intensity (EFI) distribution in the MLD stack [21–23]. To improve LIDT, different methods were explored such as a selection of materials with the highest intrinsic LIDT and/or an optimization of the stack design. Apfel *et al.* demonstrated an improvement of the LIDT by shifting EFI peaks into the most resistant material [24]. Previous works evidenced that optimizing only the outer layers can lead to a significant improvement of LIDT [25–27]. It was also reported that some designs could be very sensitive to manufacturing errors. Chorel *et al.* presented a Robust-Optimization Algorithm ROA of MLD coatings by taking into account manufacturing errors [28]. An improvement of the LIDT has been demonstrated by depositing three designs. The efficiency of the algorithm has been validated experimentally with an increase of approximately 44% between one classical design based on Quarter-Wave Optical Thickness (QWOT) and an optimized design based on the ROA [29]. As a follow-up to this study, the questions we want to answer are:

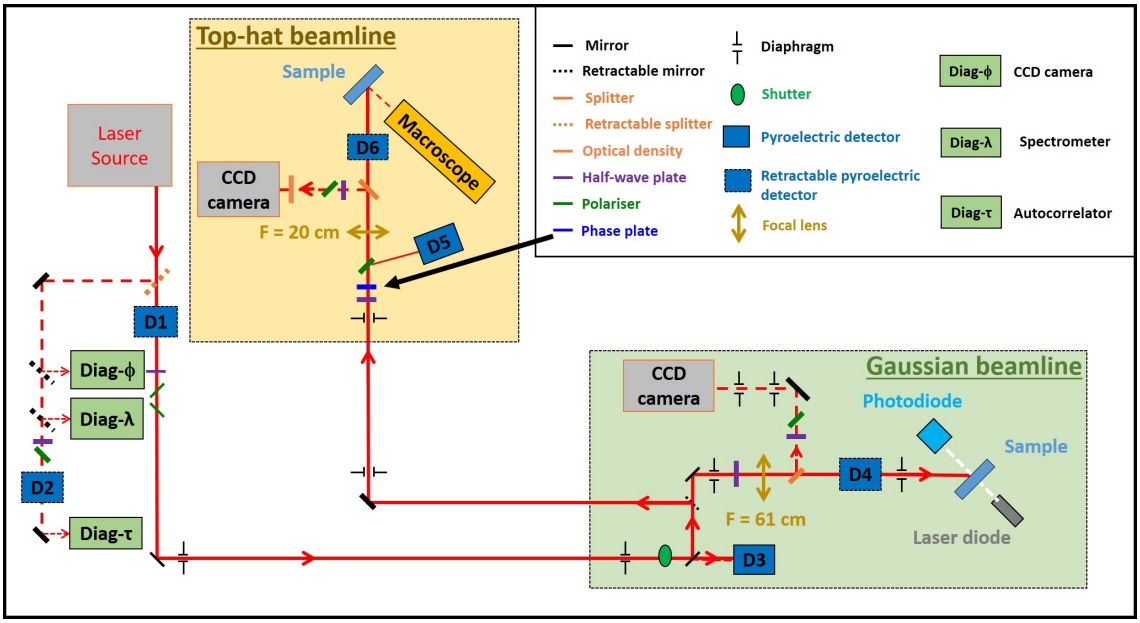

Fig. 1. Representation of the DERIC test bench.

does an increase of LIDT lead to an increase of the growth threshold and do MLD designs have an influence on damage growth rates?

To continue with the experimental validation of ROA, we investigate the improvement of Laser-Induced Damage Growth Threshold (LIDGT) along with the initiation threshold. In this paper, we present the experimental damage test bench used for the measurement of initiation threshold and damage growth experiments. Then, the designs of the three mirror samples are detailed and the results of damage growth experiments are presented. We used a spatially top-hat beam to illuminate damage sites initiated intrinsically. LIDGT and damage growth coefficients were measured to compare the damage growth dynamics of the three samples. Finally, a numerical model in 2D with the Finite Element Method (FEM) was developed to assess the trends observed experimentally.

2. EXPERIMENTAL SET-UP

The experimental study was performed on the laser test bench called DERIC at CEA-CESTA using a S-pulse Amplitude Systèmes Laser source. This laser operates at 1053 nm and delivers 2 mJ pulses at 10 Hz. The pulse duration was chosen to be as short as possible around 800 fs, estimated from the measurement of a recurrent autocorrelator [30, 31]. On this facility, two different and separated measurement beam-lines have been developed. A scheme of the set-up and of the two beam-lines is reported in Fig.1.

First, a spatially Gaussian beam is used to determine precisely the intrinsic LIDT of the optical components. Second, a square and top-hat beam is used to perform experimental growth measurements. A retractable mirror makes it easy to switch from one beam-line to another. Regarding LIDT measurements, the 1-on-1 procedure was used to assess initiation damage thresholds, intrinsic to the structure and the materials, and to discriminate which mirror exhibits the highest damage threshold [30]. In the sample plane, the Gaussian shaped focused spot has a 160 μm diameter at 1/e. On this beam-line, taking into account the error margin of each instrument, absolute fluence is given with an accuracy better than 10%. Damage detection is firstly estimated *in-situ* by means of a probe beam coupled to a Schlieren technique. Next, the occurrence of the damage is checked and validated post-mortem by means of a differential interference contrast (DIC) microscope (50× magnification) as recommended by the ISO standard [32]. This measurement beam-line is chosen to precisely measure the LIDT because the Gaussian spatial beam profile makes it possible to accurately determine the maximum beam fluence which is attributed to each laser irradiation. On the other hand, to perform accurate damage growth measurements, a homogeneous energy distribution deposited on the damage site is preferable [33]. In this way, analysis of the results is facilitated by decorrelating the laser damage dynamics from the fluence distribution of the beam. Thus, growth experiments have been carried out with a spatially square and top-hat beam. This profile is obtained by shaping the spatially Gaussian beam from the laser source with a silica phase plate associated with a 300 mm focal lens. This leads to a 150 μm squared top-hat beam at a specific position along the beam propagation axis. With the maximum energy available on the sample around 2.0 mJ, the maximum fluence is around 8.0 J/cm^2 at the plateau of the top-hat beam. The process used for the damage growth experiments has been first described in [34]. In a few words, a high peak fluence profile is first used to trigger initial damage on the dielectric mirror. Then the sample is moved along the propagation axis to the top-hat position and the growth of this initial damage site is realized by irradiating it with the top-hat profile. A microscope coupled to a camera enables both observations, the growth sequence and recording of the whole sequence. The camera is synchronized with the laser shot repetition frequency to capture, shot by shot, the evolution of the damaged area. Thanks to the microscope acquisitions, damaged areas are estimated through image processing (using Image J software) that allows to determine the growth damage rate of each damage site.

3. CHARACTERISTICS OF THE THREE DEPOSITED DESIGNS

In this study, three different mirrors have been studied. These mirrors were developed during a previous study to assess the influence of the thickness of some layers of the MLD stack to improve the LIDT of the mirrors [28].

Indeed, as described in the introduction of this paper, the LIDT of MLD coatings subjected to sub-picosecond laser pulses depends on the intrinsic laser damage threshold of the materials ($LIDT_{int}$) and the Electric Field Intensity (EFI) distribution in the stack [8]. The EFI is defined as the square norm of the electric field normalized by the square norm of the incident electric field: $EFI = |E|^2 \ / \ |E_0|^2$. Laser induced-damage will initiate where the experimental fluence modulated by the EFI is higher than the intrinsic LIDT of the material. Consequently, the LIDT of a layer can be defined as : $LIDT_{layer} = LIDT_{int} \times EFI_{max}$ where EFI_{max} represents the maximum EFI value in the layer. Then the LIDT of a multilayer is defined as the minimal LIDT value of its constituent layers. With this description, one can see that a way to increase the LIDT of mirrors is to modify the stack structure in order to adjust the EFI_{max}.

The mirror design is composed of an odd number of QWOT layers starting and finishing with the high refractive index material ($[HL]^n$ H). Having the high index material as outer layer compared to low index material increases the refractive index contrast of the first interface of the mirror with the incident medium, air. Higher the index contrast induces higher reflectivity of this interface consequently less electric field is propagating in the stack. Moreover, thick low index overcoat (2L overcoat) usually used on ns high power laser facilities transport mirrors are hosting high EFI peak value. In the present context, it is then interesting to remove this overcoat layer. The EFI of a $[HL]^n$ H design has its highest value at the interface between the two outer layers of the MLD stack. Apfel has shown that by modifying the thicknesses of those two outer layers, the EFI peak could be moved into the most resistant of the two materials which should increase the LIDT [24]. This shift is induced by increasing the thickness of the low refractive index and most resistive layer, and decreasing the thickness of the other layer. Based on this consideration, Chorel *et al.* have developed a Robust Optimization Algorithm (ROA) that modifies several layers and takes into account the manufacturing errors [28]. The number of layers to optimize is set as an input parameter of the method. Other input parameters of the ROA are the refractive indexes and the intrinsic LIDT of the materials involved in the stack. Experimental validation of this ROA method has previously shown an improvement of 44% of the LIDT [29].

To investigate the influence of coating mirror designs and the improvement of the LIDT on the laser damage growth phenomenon, we performed damage growth characterization on three different designs counting the same odd number of layers (37), all composed of hafnia and silica layers deposited on identical high damage threshold BK7 substrates by unassisted electron beam evaporation and in the same coater. The first design called **QWOT** is a mirror composed of quarter-wave optical thickness layers. The second design called **AOD** is inspired by one of the Apfel approaches described above, where the thicknesses of two outer layers are modified and weighted (balanced) by the intrinsic LIDT of the materials. The last design called **ROAD**, calculated with the ROA method has its 12 outer layers modified. All 3 mirrors are designed to provide a reflectivity higher than 99% for s and p-polarized beam at 1053 nm with an angle of incidence of 45° and for ambient air.

4. LIDT MEASUREMENTS

Designs	*p*-polarization		*s*-polarization	
	EFI	LIDT (J/cm^2)	EFI	LIDT (J/cm^2)
QWOT	1.03	2.73 ± 0.20	0.70	4.36 ± 0.31
AOD	0.85	3.83 ± 0.18	0.49	6.12± 0.11
ROAD	0.67	3.84 ± 0.43	0.43	6.12 ± 0.16

Table 1. Results of 1-on-1 damage tests performed on the three mirror designs.

First, the intrinsic LIDT of each material deposited as monolayer was measured with 1-on1 tests at normal incidence. The intrinsic LIDT values were determined at 6.23 ± 0.13 J/cm^2 and 3.08 ± 0.10 J/cm^2 for SiO_2 and HfO_2 respectively. Then, the LIDT values of all three designs were measured, as exposed in section 2, on the "Gaussian" beam-line using the 1-on-1 procedure at 45° of incidence, 0.8 ps of pulse duration, in ambient air for s- and p-polarization. Results are reported in Tab.1. Similar LIDTs were measured for both polarizations, on optics coated with the AOD and the ROAD. Lower EFI values induce higher LIDTs in s-polarization than in p-polarization. Those LIDTs are approximately 40% higher than the LIDT values of the QWOT design which confirms that optimizing the thicknesses of the outer layers increases the LIDT.

5. DAMAGE GROWTH EXPERIMENTS

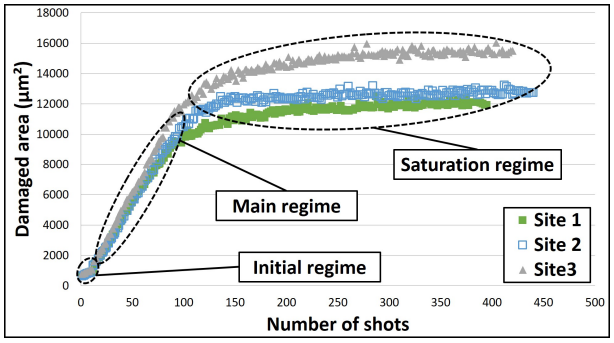

Fig. 2. Evolution of the damaged area as a function of the number of shots. Three sites have been illuminated under the same conditions at a fluence of 2.84 J/cm^2 in s-polarization. The experiments were carried out on the AOD sample.

Laser induced-damage growth experiments were performed on the "Top-hat" beam-line. First, initial damage sites were created intrinsically with a Gaussian beam at a fluence 10% above the LIDT (with a single shot). The initial damage sites have an elliptical form with a major axis diameter between 25 and 30 μm (see Fig.3(#1)). Those damage sites were illuminated with successive laser shots with the top-hat beam at different fluences (see Fig.2 and Fig.3). For a given fluence, 3 different sites were illuminated under the same conditions. The evolution of the area of the damage sites, as illustrated in Fig.2, revealed a

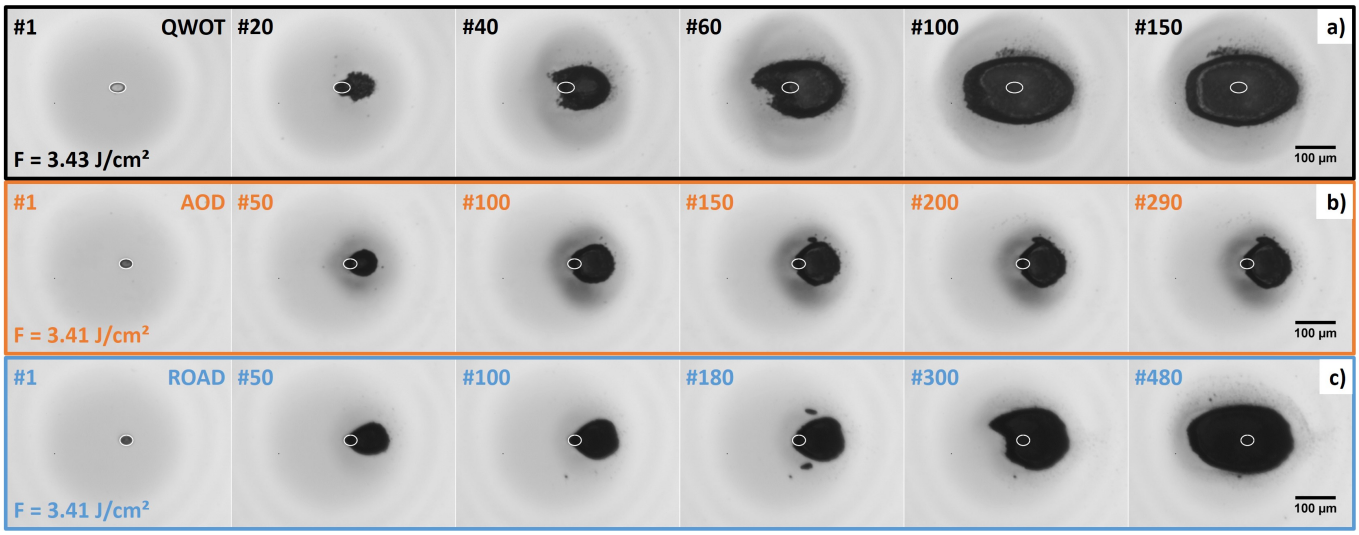

Fig. 3. Microscope acquisitions of the evolution of the damaged area. Damage growth experiments were performed on (a) QWOT design, (b) AOD, and (c) ROAD at a fluence of approximative 3.41 J/cm^2 in *s*-polarization. See Visualization 1 for complete sequences.

good repeatability of the damage growth phenomenon between different sites illuminated under the same conditions.

The results evidence three growth regimes: an initial regime with a limited evolution of the size of the damage site, a main regime with a linear evolution of damaged area, and a saturation regime which corresponds to a decrease of the damage growth until stabilization of the size of the damage sites. These three regimes were described in ref.[33]. In this case, the duration of the initial regime (number of shots) was very short for the three mirror designs (around 50 shots).Damage growth coefficients were measured by only considering the main regime, described with the following affine relationship [34–36]:

$$S_N = \beta \times N + S_0. \quad \textbf{(1)}$$

where S_N (μm^2) represents the damaged area after N shots, β (μm^2/shot) is the linear damage growth coefficient and S_0 (μm^2) represents the initial size of the damage site. For the 3 sites illuminated under the same conditions, the average between the 3 measured β coefficients is reported for each fluence.

The influence of the polarization on the damage growth phenomenon has been studied in ref.[37]. Damage growth thresholds (LIDGT), damage growth rate, and damage site morphology have been shown to depend on polarization. Figure 4 shows the evolution of the damage growth coefficients β as a function of the fluence for the three different mirror designs. LIDGT is defined as the average deviation between the highest fluence with the growth coefficient β equal to 0 and the lowest fluence with a non-zero growth coefficient. LIDGT values of the three different designs are reported in Tab.2.

In the case of *p*-polarization, LIDGT for the QWOT design is equal to 1.27 $\pm$ 0.04 J/cm^2 and for the AOD is equal to 2.11 $\pm$ 0.01 J/cm^2. The highest LIDGT is found for the ROAD at 2.35 $\pm$ 0.03 J/cm^2. This evidences an increase of the damage growth threshold between the QWOT and the two optimized designs, which can also be seen in Fig.4(a). It represents an increase of approximately 66% and 85% of the LIDGT from QWOT to AOD and QWOT to ROAD respectively. These improvements are higher than that observed for the LIDT. However, the damage growth rate seems similar for the three mirrors.

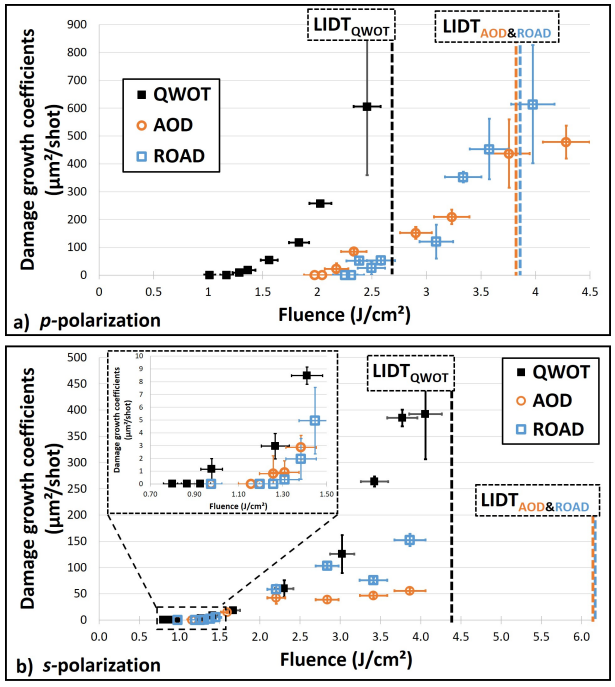

Fig. 4. Evolution of the damage growth coefficients as a function of the fluence for the three mirror designs for (a) *p*-polarization and (b) *s*-polarization. Vertical error bars represent the standard deviation between the three measured coefficients on different sites on the same sample under the same illumination conditions and fluence. The inset in figure (b) shows a zoom of the chart between 0.5 and 1.5 J/cm^2. Vertical dashed lines represent the LIDT of each mirror designs.

In the case of *s*-polarization, the results demonstrated also an improvement of the LIDGT as illustrated in the inset of Fig.4(b). We determined an improvement of approximately 29% and 35% of the LIDGT between QWOT-AOD and QWOT-ROAD respectively, which is lower compared to the improvement of the LIDT

(40%). The damage growth rate seems to be influenced by the mirror design. Under low fluences, damage growth coefficients for the three designs show values close to each other. Above a fluence of 2.50 J/cm^2, the damage growth coefficients of the QWOT design are higher than for the two optimized designs. Furthermore, the AOD has damage growth coefficients lower than the ROAD. The increase of the LIDT leads to an improvement of the LIGDT that depends on the polarization

Designs	**LIDGT** (J/cm^2)	
	p-polarization	*s*-polarization
QWOT	1.27 ± 0.04	0.95 ± 0.03
AOD	2.11 ± 0.01	1.23 ± 0.04
ROAD	2.35 ± 0.03	1.28 ± 0.04

Table 2. Measurements of damage growth thresholds on the three design mirrors.

6. MODELING OF THE DAMAGE GROWTH PHENOMENON

A 2D model using Finite Element Method (FEM) to solve the Maxwell's equations was developed to simulate damage growth sequences, as described in ref. [33]. The model is based on the hypothesis of a growth phenomenon linked to the Electric Field Intensity (EFI) in the MLD structure. The main goal of this model is to assess the different trends observed experimentally. To simulate damage mechanisms, the EFI distribution is calculated with an initial damage site in the first layer of the mirror design. Where the incident fluence modulated by the EFI reaches the intrinsic LIDT of the material, the value of the refractive index is replaced by the refractive index of air. The model is restarted with the new damaged structure.

The three mirror designs were implemented in the model. The dimension of the geometry was set to 400×9.6 μm^2. The 400 μm length corresponds to the field of view of the microscope during the experiments. The 9.6 μm corresponds approximately to the total thickness of the mirrors with 1 μm of air and substrate domain thickness. The geometry is meshed with a maximum cell size equal to $\lambda/10$ (λ corresponds to 1053 nm). Damage growth sequences at different fluences were performed only in *s*-polarization since a 3D model is needed to simulate damage growth sequences in *p*-polarization [37]. Damage growth sequences are set to have 200 iterations. At the end of the iterative process, the length of the damage site in the top layer is measured, and compared to the damaged length observed experimentally (see Fig.5(a)). The evolution of the length of the damage site revealed similar trends as observed experimentally with three growth regimes, illustrated in Fig.5(b). We considered only the main regime to measure linear damage growth coefficients based on this relation [33]:

$$L_N = \alpha \times N + L_0. \quad \textbf{(2)}$$

L_N (μm) represents the damaged length after N shots, α (μm/shot) is the linear damage growth coefficient and L_0 (μm) represents the initial damaged length.

Figure 6 represents the damage growth coefficients calculated numerically for each mirror design. The model reveals an improvement of the LIDGT between the QWOT design and the optimized designs as observed experimentally. The model evidences different damage growth rates for the mirror designs (see Fig.5(b)). A stronger damage growth rate was calculated for the QWOT design. In addition, lower damage growth coefficients were evidenced for the AOD than for the ROAD as observed experimentally. This result motivates to the study the influence of mirror designs on damage growth phenomenon more broadly. These trends revealed by the numerical calculations are consistent with the experimental observations.

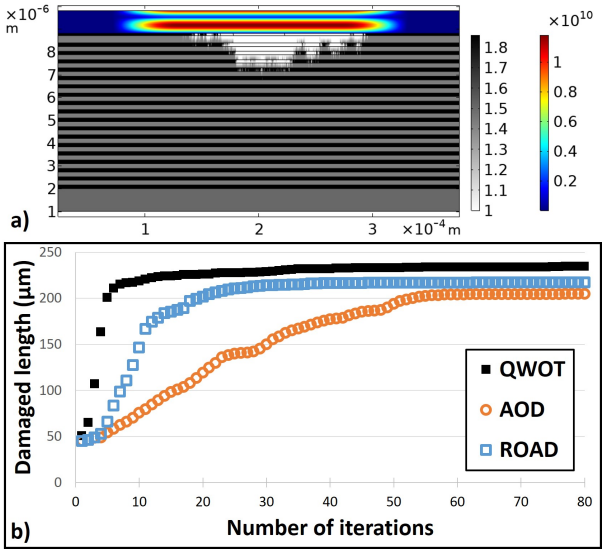

Fig. 5. (a) Example of a numerical damage growth sequence on the AOD after 15 iterations with an incident fluence of 3.8 J/cm^2 in *s*-polarization.The color scale represents the intensity of the incident beam, the gray scale represents the refraction index. (b) Evolution of length of the damage site through the entire sequence for the three mirror designs at a fluence of 3.3 J/cm^2. Only the first 80 of the 200 iterations are displayed.

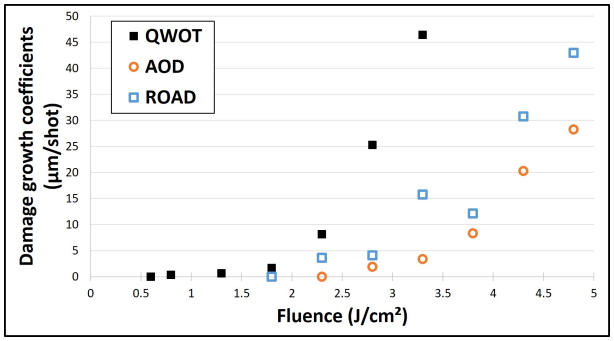

Fig. 6. Evolution of numerical damage growth coefficients in *s*-polarization as a function of the fluence following the three mirror designs.

7. CONCLUSION

The experimental results revealed an improvement of 40% of LIDT between the classical and the two optimized designs. Damage growth experiments were performed on these mirrors to measure the damage growth threshold in the two linear polarization states. The results showed an improvement of the growth

threshold between 29% and 85% depending on the polarization state.In the case of *s*-polarization, a reduction in damage growth rate is evidenced as a function of mirror designs, particularly between AOD and ROAD while similar initiation and growth thresholds have been measured. These results reveal the influence of the mirror design on the damage growth phenomenon. A 2D FEM model was used to assess the trends observed experimentally. The numerical results demonstrated similar trends to that observed experimentally with an improvement of the LIDGT between the QWOT and the two optimized designs. The numerical model was developed to validate experimental trends. It cannot to be fully representative and completely accurate first, because we cannot compare damaged length against damaged area and second the numerical model takes into account only the electric field intensity distribution. To improve the representativeness of the simulation, a 3D model including different laser damage process such as the incubation phenomenon and the deposition of debris should be developed. In addition, lower numerical damage growth coefficients were calculated with the AOD than with the other two designs. To conclude, an improvement of the initiation threshold through a modification of the mirror design can lead to a reduction of the damage growth phenomenon. These results underline the possibility of an optimization of MLD designs by taking into account the growth phenomenon.

Disclosures. The authors declare no conflicts of interest.

Acknowledgment. Portions of this work were presented at the Optical Interference Coatings in 2022, Th.D2 "Laser damage growth experiments on optimized multilayer dielectric coatings in the sub-picosecond regime".

We would like to thank the Optical Manufacturing shop group and the Optical Materials Technology group of the Laboratory for Laser Energetic for supplying the mirror samples and their interest in developing these mirrors.

Data availability. Data underlying the results presented in this paper are not publicly available at this time but may be obtained from the authors upon reasonable request.

REFERENCES

1. D. Strickland and G. Mourou, "Compression of amplified chirped optical pulses," Opt. Commun. **55**, 447 – 449 (1985).
2. T. A. Laurence, D. A. Alessi, E. Feigenbaum, R. A. Negres, S. R. Qiu, C. W. Siders, T. M. Spinka, and C. J. Stolz, "Mirrors for petawatt lasers: Design principles, limitations, and solutions," J. Appl. Phys. **128**, 071101 (2020).
3. D. Ristau, M. Jupé, and K. Starke, "Laser damage thresholds of optical coatings," Thin Solid Films **518**, 1607–1613 (2009). Proceedings of the 36th International Conference on Metallurgical Coatings and Thin Films.
4. M. D. Perry, B. C. Stuart, P. S. Banks, M. D. Feit, V. Yanovsky, and A. M. Rubenchik, "Ultrashort-pulse laser machining of dielectric materials," J. Appl. Phys. **85**, 6803–6810 (1999).
5. B. C. Stuart, M. D. Feit, A. M. Rubenchik, B. W. Shore, and M. D. Perry, "Laser-induced damage in dielectrics with nanosecond to subpicosecond pulses," Phys. Rev. Lett. **74**, 2248–2251 (1995).
6. L. A. Emmert, M. Mero, and W. Rudolph, "Modeling the effect of native and laser-induced states on the dielectric breakdown of wide band gap optical materials by multiple subpicosecond laser pulses," J. Appl. Phys. **108**, 043523 (2010).
7. M. Mero, J. Liu, W. Rudolph, D. Ristau, and K. Starke, "Scaling laws of femtosecond laser pulse induced breakdown in oxide films," Phys. Rev. B **71**, 115109 (2005).
8. L. Gallais and M. Commandré, "Laser-induced damage thresholds of bulk and coating optical materials at 1030 nm, 500 fs," Appl. Opt. **53**, A186–A196 (2014).
9. M. Mero, B. R. Clapp, J. C. Jasapara, W. G. Rudolph, D. Ristau, K. Starke, J. Krüger, S. Martin, and W. Kautek, "On the damage behavior of dielectric films when illuminated with multiple femtosecond laser pulses," Opt. Eng. **44**, 051107 (2005).
10. A. A. Kozlov, J. C. Lambropoulos, J. B. Oliver, B. N. Hofman, and S. Demos, "Mechanisms of picosecond laser-induced damage in common multilayer dielectric coatings," Sci. Reports **9**, 607 (2019).
11. D. Ashkenasi, M. Lorenz, R. Stoian, and A. Rosenfeld, "Surface damage threshold and structuring of dielectrics using femtosecond laser pulses: the role of incubation," Appl. Surf. Sci. **150**, 101–106 (1999).
12. L. Gallais, X. Cheng, and Z. Wang, "Influence of nodular defects on the laser damage resistance of optical coatings in the femtosecond regime," Opt. Lett. **39**, 1545–1548 (2014).
13. O. Favrat, M. Sozet, I. Tovena-Pécault, L. Lamaignère, and J. Néauport, "Influence of organic contamination on laser induced damage of multilayer dielectric mirrors by subpicosecond laser pulses," in *Laser-Induced Damage in Optical Materials: 2014,* vol. 9237 G. J. Exarhos, V. E. Gruzdev, J. A. Menapace, D. Ristau, M. Soileau, and D. Ristau, eds., International Society for Optics and Photonics (SPIE, 2014), pp. 35 – 40.
14. A. Hervy, L. Gallais, D. Mouricaud, G. Chériaux, O. Utéza, R. Clady, M. Sentis, and A. Fréneaux, "Thin films characterizations to design high-reflective coatings for ultrafast high power laser systems," in *Laser-Induced Damage in Optical Materials: 2014,* vol. 9237International Society for Optics and Photonics (SPIE, 2014), pp. 59 – 65.
15. T. A. Laurence, R. A. Negres, S. Ly, N. Shen, C. W. Carr, D. A. Alessi, A. Rigatti, and J. D. Bude, "Role of defects in laser-induced modifications of silica coatings and fused silica using picosecond pulses at 1053 nm: Ii. scaling laws and the density of precursors," Opt. Express **25**, 15381–15401 (2017).
16. Y. Cui, Y. Zhao, H. Yu, H. He, and J. Shao, "Impact of organic contamination on laser-induced damage threshold of high reflectance coatings in vacuum," Appl. Surf. Sci. **254**, 5990 – 5993 (2008).
17. K. R. P. Kafka and S. G. Demos, "Interaction of short laser pulses with model contamination microparticles on a high reflector," Opt. Lett. **44**, 1844–1847 (2019).
18. M. Sozet, S. Bouillet, J. Berthelot, J. Neauport, L. Lamaignère, and L. Gallais, "Sub-picosecond laser damage growth on high reflective coatings for high ower applications," Opt. Express **25**, 25767 (2017).
19. Y. Hao, M. Sun, Z. Jiao, Y. Guo, X. Pan, X. Pang, and J. Zhu, "Determination of the damage growth threshold of multilayer dielectric gratings by picosecond laser pulses based on saturation damage size analysis," Appl. Opt. **57**, 4191–4201 (2018).
20. M. A. Norton, E. E. Donohue, M. D. Feit, R. P. Hackel, W. G. Hollingsworth, A. M. Rubenchik, and M. L. Spaeth, "Growth of laser damage on the input surface of SiO2 at 351 nm," in *Laser-Induced Damage in Optical Materials: 2006,* vol. 6403 G. J. Exarhos, A. H. Guenther, K. L. Lewis, D. Ristau, M. J. Soileau, and C. J. Stolz, eds., International Society for Optics and Photonics (SPIE, 2007), pp. 210 – 218.
21. M. Chorel, S. Papernov, A. A. Kozlov, B. N. Hoffman, J. B. Oliver, S. G. Demos, T. Lanternier, E. Lavastre, L. Lamaignère, N. Roquin, B. Bousquet, N. Bonod, and J. Néauport, "Influence of absorption-edge properties on subpicosecond intrinsic laser-damage threshold at 1053 nm in hafnia and silica monolayers," Opt. Express **27**, 16922–16934 (2019).
22. J. Neauport, E. Lavastre, G. Razé, G. Dupuy, N. Bonod, M. Balas, G. de Villele, J. Flamand, S. Kaladgew, and F. Desserouer, "Effect of electric field on laser induced damage threshold of multilayer dielectric gratings," Opt. Express **15**, 12508–12522 (2007).
23. G. Abromavicius, R. Buzelis, R. Drazdys, A. Melninkaitis, and V. Sirutkaitis, "Influence of electric field distribution on laser-induced damage threshold and morphology of high-reflectance optical coatings," in *Laser-Induced Damage in Optical Materials: 2007,* vol. 6720 G. J. Exarhos, A. H. Guenther, K. L. Lewis, D. Ristau, M. J. Soileau, and

C. J. Stolz, eds., International Society for Optics and Photonics (SPIE, 2007), pp. 329 – 336.

24. J. H. Apfel, "Optical coating design with reduced electric field intensity," Appl. Opt. **16**, 1880–1885 (1977).
25. H. Becker, D. Tonova, M. Sundermann, L. Jensen, M. Gyamfi, D. Ristau, and M. Mende, "Advanced femtosecond laser coatings raise damage thresholds," in *Optical Systems Design 2015: Advances in Optical Thin Films V,* vol. 9627 M. Lequime, H. A. Macleod, and D. Ristau, eds., International Society for Optics and Photonics (SPIE, 2015), pp. 215 – 220.
26. S. Chen, Y. Zhao, Z. Yu, Z. Fang, D. Li, H. He, and J. Shao, "Femtosecond laser-induced damage of hfo2/sio2 mirror with different stack structure," Appl. Opt. **51**, 6188–6195 (2012).
27. T. Willemsen, M. Jupé, M. Gyamfi, S. Schlichting, and D. Ristau, "Enhancement of the damage resistance of ultra-fast optics by novel design approaches," Opt. Express **25**, 31948–31959 (2017).
28. M. Chorel, T. Lanternier, Éric Lavastre, N. Bonod, B. Bousquet, and J. Néauport, "Robust optimization of the laser induced damage threshold of dielectric mirrors for high power lasers," Opt. Express **26**, 11764–11774 (2018).
29. M. Chorel, T. Lanternier, Éric Lavastre, B. Bousquet, N. Bonod, J. B. Oliver, A. L. Rigatti, A. A. Kozlov, B. N. Hoffman, S. G. Demos, J. Daurios, and J. Néauport, "Experimental validation of the robust optimization algorithm for high-fluence optical coatings," in *Optical Interference Coatings Conference (OIC) 2019,* (Optica Publishing Group, 2019), p. ThA.5.
30. A. Ollé, J. Luce, N. Roquin, C. Rouyer, M. Sozet, L. Gallais, and L. Lamaignère, "Implications of laser beam metrology on laser damage temporal scaling law for dielectric materials in the picosecond regime," Rev. Sci. Instruments **90**, 073001 (2019).
31. Y. Takagi, T. Kobayashi, K. Yoshihara, and S. Imamura, "Multiple- and single-shot autocorrelator based on two-photon conductivity in semiconductors," Opt. Lett. **17**, 658–660 (1992).
32. *ISO Standard Nos 21254-1–21254-4* (2011).
33. S. Diop, A. Ollé, N. Roquin, M. Chorel, Éric Lavastre, L. Gallais, N. Bonod, and L. Lamaignère, "Investigation of the influence of a spatial beam profile on laser damage growth dynamics in multilayer dielectric mirrors in the near infrared sub-picosecond regime," Opt. Express **30**, 17739–17753 (2022).
34. A. Ollé, S. Diop, N. Roquin, L. Gallais, and L. Lamaignère, "Temporal dependency in the picosecond regime of laser damage growth," Opt. Lett. **45**, 4024–4027 (2020).
35. M. Sozet, J. Neauport, E. Lavastre, N. Roquin, L. Gallais, and L. Lamaignère, "Laser damage growth with picosecond pulses," Opt. Lett. **41**, 2342–2345 (2016).
36. Y. Hao, M. Sun, Y. Guo, S. Shi, X. Pan, X. Pang, and J. Zhu, "Asymmetrical damage growth of multilayer dielectric gratings induced by picosecond laser pulses," Opt. Express **26**, 8791–8804 (2018).
37. S. Diop, M. Chorel, A. Ollé, N. Roquin, Éric Lavastre, L. Gallais, N. Bonod, and L. Lamaignère, "Polarization dependence of laser damage growth features on multilayer dielectric mirrors for petawatt-class lasers," Opt. Lett. **47**, 6177–6180 (2022).